Iranian Journal of Numerical Analysis and Optimization

Vol. ??, No. ??, ??, pp ??

https://doi.org/??

https://ijnao.um.ac.ir/





Research Article



A study on efficient chaotic modeling via fixed-memory length fractional Gauss maps

A. Bellout, R. Bououden, S.E.I. Bouzeraa and M. Berkal*, [©]



*Corresponding author

Received ????; revised ???; accepted ???

Aida Bellout

Laboratory of Mathematics and their Interactions, Department of Mathematics, Abdelhafid Boussouf University Center, Algeria. e-mail: a.bellout@centre-univ-mila.dz

Rabah Bououden

Laboratory of Mathematics and their Interactions, Department of Mathematics, Abdelhafid Boussouf University Center, Algeria.

Department of Applied Mathematics, Abdelhafid Boussouf University Center, Mila ,R.P 26, Mila, 43000, Algeria. e-mail: r.bouden@centre-univ-mila.dz

Seyf El Islam Bouzeraa

Department of Applied Mathematics, Abdelhafid Boussouf University Center, Mila, R.P 26, Mila, 43000, Algeria. e-mail: s.bouzeraa@centre-univ-mila.dz

Messaoud Berkal

Department of Applied Mathematics, Abdelhafid Boussouf University Center, Mila ,R.P 26, Mila, 43000, Algeria. e-mail: m.berkal@centre-univ-mila.dz

How to cite this article

Bellout, A., Bououden, R., Bouzeraa, S.E.I. and Berkal, M., A study on efficient chaotic modeling via fixed-memory length fractional Gauss maps. *Iran. J. Numer. Anal. Optim.*, ??; ??(??): ??-??. ??

This paper investigates the dynamic behavior of the fractional Gauss map with fixed memory length, highlighting its potential for efficient chaotic modeling. Unlike classical fractional systems that require the full history of states, the proposed approach introduces a memory-limited version, significantly reducing computational cost while preserving complex dynamical features. Through bifurcation analysis, Lyapunov exponents, and the 0-1 test for chaos, the study demonstrates that the system exhibits a rich variety of behaviors, including periodic, quasi-periodic, and chaotic regimes, depending on the fractional order and memory size. A comparative evaluation with the classical Gauss map reveals that the fixed-memory model retains similar chaotic characteristics, but with improved computational efficiency. These findings suggest that fixed-memory fractional maps offer a practical alternative for simulating chaotic systems in real-time applications.

AMS subject classifications (2020): Primary 39A33; Secondary 37D45, 37N30.

Keywords: Chaos; Fractional difference equations; Gauss map; Fixed memory length; Bifurcation; Lyapunov exponent.

1 Introduction

Chaotic systems play a fundamental role in the modeling and analysis of non-linear dynamics across various disciplines, including mathematics, physics, biology, engineering and optimization [3, 4, 5, 7, 6, 8, 11, 10, 12, 13, 14, 15, 24, 26, 27, 25]. During this period, several chaotic discrete systems have been proposed, such as the Logistic map, Tent map, Gauss map, Hénon map, and Lozi map [21, 23, 28, 35, 37, 39].

The Gauss map, in particular, has been widely studied due to its rich and sensitive dependence on initial conditions, making it a valuable tool for exploring chaotic behavior in discrete systems [39]. In parallel, the theory of fractional-order systems has gained increasing attention over the past two decades as an effective framework for modeling systems with memory and hereditary properties [17, 16, 31, 32, 41]. Fractional difference equations provide a generalization of traditional difference equations, allowing the present state to depend on all past states with power-law weighting.

However, a significant limitation of classical fractional models lies in their requirement to store and process the entire history of the system, which can lead to high computational and memory costs. This challenge becomes especially critical in real-time simulations or large-scale systems [16, 30, 33, 41]. To overcome this issue, researchers have introduced fractional systems with fixed memory length, where only a finite number of past states contribute to the current state. This approach reduces computational complexity while preserving key dynamic features of the system [2, 18, 19]. Despite its potential, there is still a lack of comprehensive studies exploring how memory truncation affects the long-term behavior of chaotic fractional maps, particularly in comparison with both classical (nonfractional) and full-memory fractional systems.

To address these limitations, this study employs a fixed memory length approach, which restricts the influence of past states to a finite window. This strategy not only reduces computational complexity but also reflects practical constraints encountered in real-world systems. In many applications, such as real-time control systems, embedded cryptographic protocols, and biological modeling, memory and computational resources are severely limited [9, 22, 36]. For instance, control algorithms deployed on microcontrollers must operate under strict timing and memory constraints, while cryptographic systems benefit from low-latency and lightweight implementations. Similarly, in biological modeling, such as simulating cardiac activity, it is often reasonable to assume that only a limited history influences the current state due to physiological time scales. Fixed-memory fractional models thus provide a realistic and efficient alternative, balancing dynamical richness with feasibility.

This paper addresses this gap by investigating the dynamic behavior of the fractional Gauss map with fixed memory length. We employ several tools-such as bifurcation diagrams, Lyapunov exponents, and the 0-1 test to analyze the system's response under various parameter values. Additionally, we perform a comparative analysis with the classical Gauss map to evaluate the impact of fixed memory on both chaos and computational performance. The results demonstrate that the proposed model maintains the richness of chaotic dynamics while achieving improved computational efficiency, making

it a promising approach for practical applications where memory and speed are critical factors.

2 Fractional discrete-time calculus

Fractional discrete-time calculus extends classical difference equations by allowing the order of differencing to be noninteger (fractional), which makes it suitable for modeling systems with memory and hereditary properties. This is particularly useful in fields where past states influence current behavior in a gradual and persistent manner. One of the key operators used in this context is the Caputo-like delta fractional difference, introduced in [1, Definition 13]. This operator is a discrete analog of the Caputo derivative from continuous fractional calculus, and it is defined in a way that aligns naturally with initial conditions, making it more convenient for modeling real-world systems.

Let $q \in \mathbb{R}$ be fixed and let $\mathbb{N}_q = \{q, q+1, q+2, \ldots\}$ denote the isolated time scale. For the function u(n), the delta difference operator Δ is defined as follows:

$$\Delta u(n) = u(n+1) - u(n). \tag{1}$$

Definition 1. [38]

Let $u: \mathbb{N}_q \longrightarrow \mathbb{R}$ and v > 0. Then the fractional sum of order v is defined by

$$\Delta_q^{-v} u(t) = \frac{1}{\Gamma(v)} \sum_{s=q}^{t-v} (t - \sigma(s))^{(v-1)} u(s), \ t \in \mathbb{N}_{q+v}, \tag{2}$$

where q is the starting point, $\sigma(s) = s+1$ and t^v is the falling function defined in terms of the Gamma function as

$$t^{(v)} = \frac{\Gamma(t+1)}{\Gamma(t+1-v)}. (3)$$

Definition 2. [1]

For v > 0, $v \notin \mathbb{N}$ and u(t) defined on \mathbb{N}_q , the Caputo-like delta difference is defined by

$$^{c}\Delta_{q}^{v}u(t) = \Delta_{q}^{-(m-v)}\Delta^{m}u(t), \tag{4}$$

$$= \frac{1}{\Gamma(m-v)} \sum_{s=q}^{t-(m-v)} (t - \sigma(s))^{(m-v-1)}, \Delta_s^m u(s),$$
 (5)

where $t \in \mathbb{N}_{q+m-v}$ and m = [v] + 1.

Here, $\sigma(s) = s+1$ is the forward jump operator commonly used on discrete time scales. It defines the next point in the discrete domain and ensures that the summation aligns with the forward-shifted indices. This choice is standard in delta-type fractional calculus and reflects the progression of discrete time by one step. The term $(t - \sigma(s))^{(m-v-1)}$ represents the falling factorial kernel, which weights recent values more heavily than older ones, capturing the memory effect inherent in fractional systems.

Theorem 1 ([20]). For the delta fractional difference equation

$$\begin{cases} [c]c^{c}\Delta_{q}^{v}u(t) = f(t+v-1, u(t+v-1)), \\ \Delta^{k}u(q) = u_{k}, m = [v] + 1, & k = 0, \dots, m-1, \end{cases}$$

the equivalent discrete integral equation can be obtained as

$$u(t) = u_0(t) + \frac{1}{\Gamma(v)} \sum_{s=q+m-v}^{t-v} (t - \sigma(s))^{(v-1)} \times f(s+v-1, \ u(s+v-1), \ t \in \mathbb{N}_{q+m},$$
(6)

where

$$u_0(t) = \sum_{k=0}^{m-1} \frac{(t-q)^{(q)}}{k!} \Delta^k u(q).$$
 (7)

This operator calculates a fractional change in u(t), but instead of only using current and previous values (as in classical differences), it uses a weighted sum of past changes, giving more weight to recent values and less to older ones. This model is systems where recent history has a stronger effect, but the influence of earlier states still persists.

The Caputo-like delta fractional difference is chosen in this work due to several theoretical and practical advantages over other discrete fractional operators, such as the Riemann–Liouville type or Grünwald–Letnikov formulations.

First, the Caputo-like formulation allows for the use of initial conditions in the same form as those used in classical integer-order systems. This makes it more suitable for physical and biological modeling, where initial values often have direct physiological interpretations.

Second, the Caputo-like operator naturally accommodates memory effects by incorporating a weighted history of the system states, while still preserving computational tractability due to its structured definition.

Importantly, in the context of biological systems such as cardiac models, memory plays a crucial role in capturing physiological phenomena. The electrical activity of the heart, for example, is influenced not only by the current stimulus but also by a history of past activations and recovery processes. Fractional models have been shown to better replicate such long-range dependence in excitable tissues compared to their integer-order counterparts [36, 40].

The Caputo-like operator is particularly advantageous here because it reflects this hereditary behavior while maintaining a clear relationship with classical dynamics. This balance between interpretability, memory fidelity, and numerical implementation makes the Caputo-like fractional difference a compelling choice for modeling complex, memory-dependent systems like cardiac cells.

3 Fractional Gauss map with fixed memory length

In mathematics, the Gauss map, also referred to as the Gaussian map [29], is a nonlinear iterated mapping that transforms real numbers into a real interval using the Gaussian function defined as follows:

$$x_{n+1} = \exp(-ax_n^2) + b,$$
 (8)

where a and b are bifurcation parameters.

This map can exhibit chaotic behavior, for example, when a=7.5 and b=-0.6. This map is also known as the mouse map due to its bifurcation diagram when a=7.5 and b in the range -1 to 1 resembling a mouse as in Figure 1.

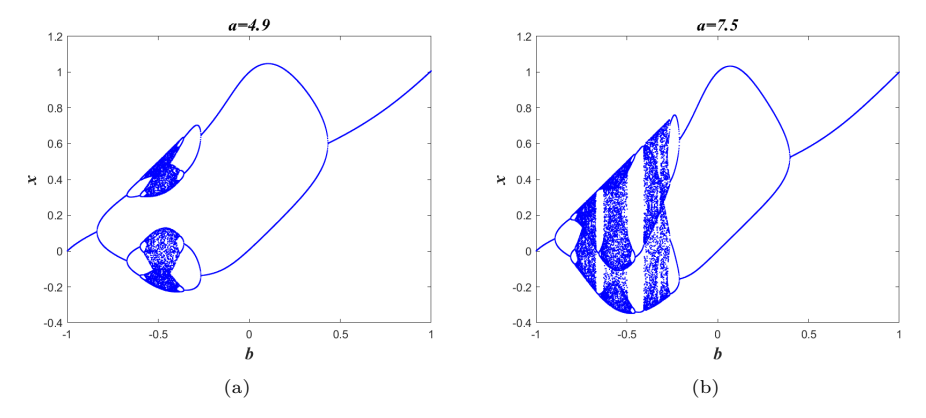


Figure 1: Bifurcation diagram of map (8) with $x_0 = 0$ and b in the range -1 to 1, (a) a = 4.9 and (b) a = 7.5

Figure 1 shows the bifurcation diagram of the fractional Gauss map (8) for two different sets of parameters: The first set is a=4.9 and b in the range -1 to 1; the second set is a=7.5 and b in the range -1 to 1.

The first-order difference of Gauss map can be easily expressed as

$$\Delta x_n = \exp(-ax_n^2) + b - x_n. \tag{9}$$

In discrete fractional calculus, the fractional Gauss map can be defined as

$$^{c}\Delta_{q}^{v}x_{n} = \exp(-ax(t-1+v)^{2}) + b - x(t-1+v),$$
 (10)

where ${}^c\Delta_q^v$ is the fractional difference of Caputo and $0 < v \le 1$ is the difference order. For the Gauss map (10), an explicit numerical solution can be given by

$$x_n = x_0 + \frac{1}{\Gamma(v)} \sum_{j=1}^n \frac{\Gamma(n-j+v)}{\Gamma(n-j+1)} (\exp(-ax(j-1)^2) + b - x(j-1)),$$
 (11)

where x_0 is initial condition.

For v = 1, the discrete fractional map (11) simplifies to the classical map (8). Unlike the integer order map (8), the fractional map (11) includes a discrete kernel function that relies on past information $x_0, x_1, \ldots, x_{n-1}$. Consequently, the memory effects in these discrete maps imply that their

current state of evolution depends on all previous states. Figure 2 shows

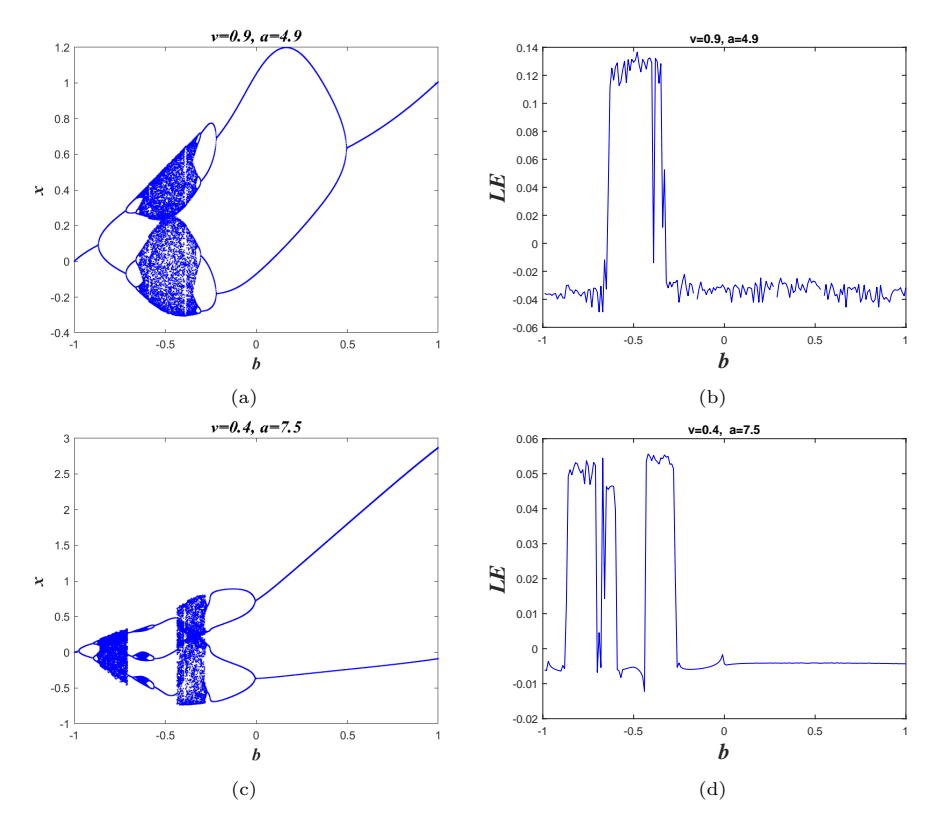


Figure 2: (a) Bifurcation diagram of fractional Gauss map (11) for v=0.9, $x_0=0$, b in the range -1 to 1 and a=4.9, (b) the greatest Lyapunov exponent of fractional Gauss map for v=0.9, $x_0=0$, b in the range -1 to 1 and a=4.9, (c) Bifurcation diagram of fractional Gauss map (11) for v=0.4, $x_0=0$, b in the range -1 to 1 and a=7.5, (d) the greatest Lyapunov exponent of fractional Gauss map for v=0.4, $x_0=0$, b in the range -1 to 1 and a=7.5.

the bifurcation diagram and Lyapunov exponent of the fractional Gauss map (11) for two different sets of parameters: The first set is a=4.9, v=0.9, and b in the range -1 to 1; the second set is a=7.5, v=0.4, and b in the range -1 to 1.

For example, for v=0.4 and a=7.5, we note that the map (11) converges to period-1 orbit for $-1 \le b < -0.97$. The first bifurcation occurs when b=-0.97, transitioning from a fixed point to a period-2 orbit via period-doubling bifurcation. Figure 2(d) confirms this information because the Lyapunov exponent is negative over the interval $-1 \le b < -0.97$ and

becomes zero when b = -0.97. The map maintains the same behavior until b = -0.89, where the second bifurcation occurs, transitioning from a period-2 orbit to a period - 4 orbit via period-doubling bifurcation. When b > -0.87, the Lyapunov exponent becomes positive, indicating that the map has become chaotic over the interval $-0.87 \le b < -0.7$; this is confirmed by Figures 2(d) and 2(c). When $-0.7 \le b < -0.67$, the map converges to a *period*-3 orbit, which further confirms that the map is chaotic for certain values of b [34]. Another bifurcation occurs when b = -0.67, transitioning from a period – 3 orbit to a period - 6 orbit via period-doubling bifurcation. Another return to chaotic behavior of the map (11) from point b = -0.66 to point b = -0.59as shown in Figure 2(c). Then, as $-0.59 \le b < -0.56$, the map (11) converges to period - 6 orbit for the second time. After that, the map (11) converges again to period - 3 orbit in the interval $-0.56 \le b < -0.43$. Again, in the interval $-0.43 \le b < -0.27$, map (11) has chaotic behavior. On the interval $-0.27 \le b < 0$, map (11) converges to period - 4 orbit again. Finally, as $0 \le b \le 1$, map (11) converges to period - 2 orbit for the second time.

It should be noted that the figure presenting the Lyapunov exponent of the map (11) confirms all previously mentioned results, where the Lyapunov exponent is negative when the orbit of map (11) converges towards a periodic orbit, is zero at the bifurcation point, and positive when the trajectory converges to chaotic behavior.

In classical fractional-order models, the system exhibits infinite memory, where all past states influence the present dynamics with a decaying weight. While this feature captures hereditary effects accurately, it leads to high computational cost and memory storage requirements, especially in long-term simulations.

To address these limitations, this study employs a fixed memory length approach, which restricts the influence of the past to a finite window of previous steps. This simplification not only reduces computational complexity but also reflects a more realistic assumption in many physical and biological systems where distant past events have negligible influence.

Moreover, the use of fixed memory enhances numerical stability and implementation efficiency, making it more suitable for real-time applications or hardware-constrained systems. In contrast, infinite memory schemes may suffer from accumulating numerical errors and impractical memory demands over long simulation horizons.

Therefore, the adoption of a fixed-memory fractional Gauss map strikes a balance between capturing essential memory effects and maintaining tractable, efficient simulations. This feature is particularly advantageous in chaotic modeling, where fast computation and sensitivity to initial conditions are critical. The following equation defines the fractional Gauss map with fixed memory length:

$$\begin{cases} x_n = x_0 + \frac{1}{\Gamma(v)} \sum_{j=1}^n \frac{\Gamma(n-j+v)}{\Gamma(n-j+1)} (\exp(-ax(j-1)^2) + b - x(j-1)) & if \quad n \le L, \\ x_n = \frac{1}{\Gamma(v)} \sum_{j=n-L}^n \frac{\Gamma(n-j+v)}{\Gamma(n-j+1)} (\exp(-ax(j-1)^2) + b - x(j-1)) & else, \end{cases}$$
(12)

where L is the length of the memory.

In classical fractional systems, the entire past state history contributes to

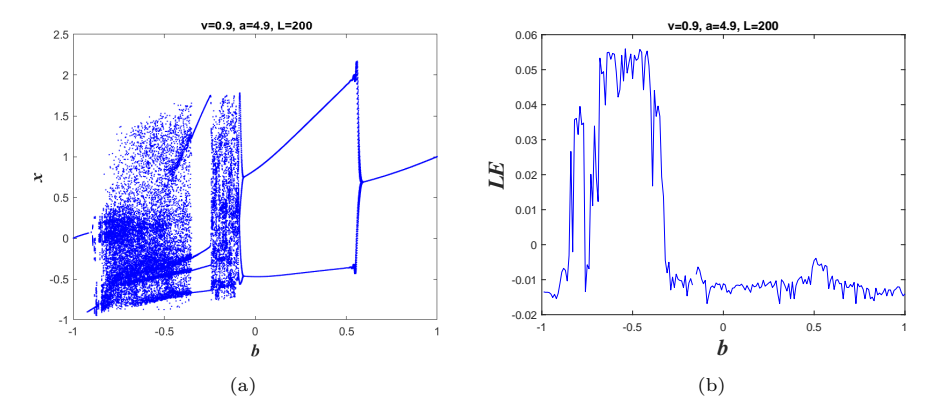


Figure 3: (a) Bifurcation diagram of the fractional Gauss map with fixed memory length for $L=200, v=0.9, x_0=0, a=4.9$ and b in the range -1 to 1, (b) The greatest Lyapunov exponent for $L=200, v=0.9, x_0=0, a=4.9$ and b in the range -1 to 1.

the current state, with memory effects governed by a power-law kernel. This long-term memory is central to capturing hereditary and complex dynamics. However, it comes at the cost of high computational demands and sensitivity to numerical errors over long simulations. The introduction of fixed memory length, denoted by L, truncates the influence of past states to only the most

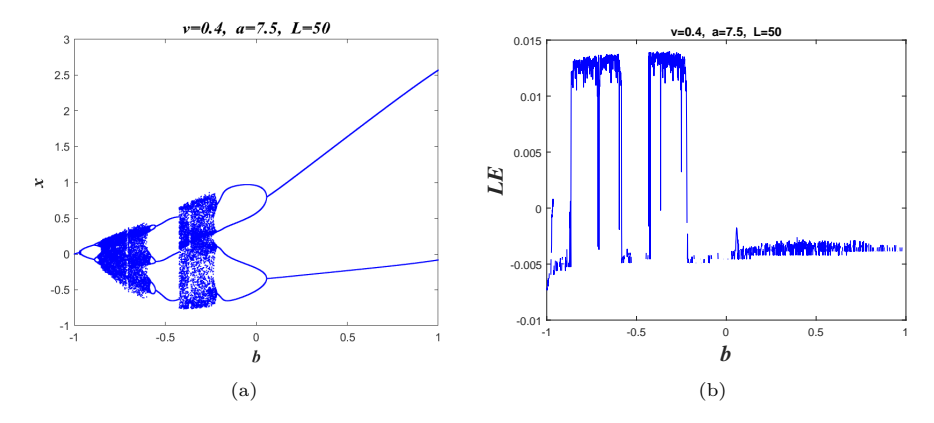


Figure 4: (a) Bifurcation diagram of the fractional Gauss map with fixed memory length for $L=50, v=0.4, x_0=0, a=7.5$ and b in the range -1 to 1, (b) The greatest Lyapunov exponent for $L=50, v=0.4, x_0=0, a=7.5$ and b in the range -1 to 1 .

recent L iterations. This simplification raises fundamental questions about how such truncation affects the nature of chaos.

Qualitatively, memory truncation can dampen long-range correlations, potentially reducing the depth of chaotic complexity or altering the sequence of bifurcations. However, as demonstrated in Figures 3 and 4, the fixed-memory fractional Gauss map continues to exhibit hallmark features of chaotic systems (including period-doubling routes to chaos, windows of periodicity, and regions of positive Lyapunov exponents) despite having a finite memory. The preservation of these structures suggests that essential nonlinear behavior remains intact even when older history is ignored.

Quantitatively, our simulations show that when comparing the full-memory fractional map (11) with the fixed-memory version (12), the **critical** bifurcation points and ranges of chaotic behavior shift only slightly, and the values of the largest Lyapunov exponents remain within comparable ranges.

Moreover, the numerical gain is substantial. Table 1 illustrates that computation time is reduced by up to 99% when memory is fixed, without sacrificing the model's ability to simulate chaos. This trade-off between **computational efficiency** and **memory fidelity** is favorable in real-time or embedded systems, where resource constraints are strict.

Table 1: The time required to obtain the path of the fractional Gauss map (FGM) and the fractional gauss map with fixed memory length (FGMFML) when L=50.

Number of iteration	FGM	FGMFML
1000	0.920305	0.205349
5000	91.580199	0.264022
10000	732.813417	0.267275
20000	13121.494701	0.304672

Figures 3 and 4 show the bifurcation diagram and Lyapunov exponent of a fractional Gauss map with fixed memory length and the greatest Lyapunov exponent for two different sets of parameters: The first set is a=4.9, v=0.9, L=200 and b in the range -1 to 1; the second set is a=7.5, v=0.4, L=50 and b in the range -1 to 1.

When comparing Figure 2, which represents the bifurcation diagram of the fractional Gauss map, with Figure 4, which represents the bifurcation diagram of the fractional Gauss map with a fixed memory length, we obtain the following observations and results:

Every feature included in the fractional order bifurcation diagram can additionally be seen in fractional order with fixed memory length bifurcation diagrams.

We can see an increase in the period of the bifurcations, which results in chaos in all bifurcation diagrams.

From the bifurcation diagram shown in Figure 4 for the fractional Gauss map with a fixed memory length L=50 we observe if $-1 \le b < -0.97$ the map (12) converges to period-1 orbit. The first bifurcation occurs when b=-0.97, transitioning from a fixed point to a period-2 orbit via period-doubling bifurcation. Figure 4(b) confirms this information because the Lyapunov exponent is negative over the interval $-1 \le b < -0.97$ and becomes zero when b=-0.97. The map maintains the same behavior until b=-0.88, where the second bifurcation occurs, transitioning from a period-2 orbit to a period-4 orbit via period-doubling bifurcation. When -0.88 < b < -0.58, the Lyapunov exponent becomes positive, indicating that the map has become chaotic over the interval -0.88 < b < -0.58; this is confirmed by Figures 4(b) and 4(a). When $-0.58 \le b < -0.55$, the map converges to a period-6 orbit, which further confirms that the map is chaotic for certain values of b. Another bifurcation

occurs when b = -0.55, transitioning from a period-6 orbit to a period-3 orbit. Another return to chaotic behavior of the map (12) from point b = -0.42 to point b = -0.21 as shown in Figure 4(a). Then, as $-0.21 \le b < -0.06$ the map (12) converges to period-4 orbit for the second time. After that, the map (12) converges again to period-2 orbit in the interval $0.06 \le b < 1$.

The figure displaying the Lyapunov exponent for map (12) validates all prior conclusions. It demonstrates that the Lyapunov exponent is negative when the orbit of map (12) approaches a periodic state, zero at the bifurcation point, and positive when the trajectory transitions into chaotic behavior.

The parameter values used in our simulations, such as a=4.9, a=7.5, and $b \in [-1,1]$, are selected based on their well-known ability to produce rich dynamical behaviors in the classical Gauss map. The fractional orders v=0.4 and v=0.9 were chosen to compare strong memory effects versus near-integer behavior. The memory lengths L=50 and L=200 were used to evaluate the impact of truncation while maintaining low computational cost.

By comparing the bifurcation diagrams of the fractional Gauss map and the fractional Gauss map with fixed memory length, we can conclude that the length of the memory has a big effect on the dynamics of the map.

We mentioned in the first section that the numerical calculation of the discrete fraction system is very time-consuming compared to the numerical calculation of the discrete fraction system with a fixed memory length, and this is what we will prove in this part through the table that summarizes the results of the time taken to obtain the path of the fractional Gauss map and the fractional Gauss map with a fixed memory length, and we used the MATLAB program and ran it on an i5 processor, 2.40GHz with 16G of RAM (random access memory).

Table 1 compares the computation time required by the fractional Gauss map with two memory strategies: Infinite memory and fixed memory length. The results clearly indicate that the fixed-memory approach significantly reduces the computational burden.

This improvement becomes more pronounced as the simulation horizon increases, highlighting the scalability of the proposed method. By limiting the number of past states involved in each iteration, the fixed-memory model avoids redundant calculations while still capturing the essential memory dynamics of the system.

Such a reduction in execution time is crucial for real-time applications and long-term simulations, especially in hardware-constrained environments or large-scale systems. Therefore, the use of fixed memory not only enhances numerical efficiency but also makes the fractional modeling of chaotic systems more practical and accessible.

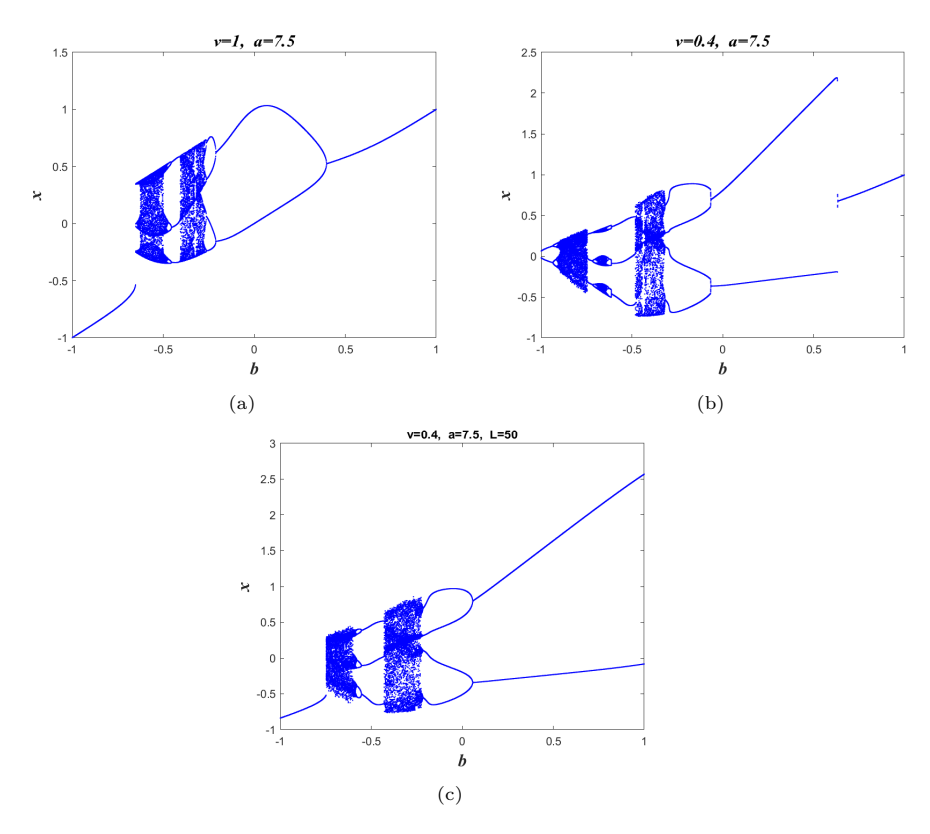


Figure 5: Bifurcation diagram of fractional gauss map with initial condition as $x_0 = 0.9$ and b in the range -1 to 1 where, (a)for v = 1, (b) for v = 0.4 and (c) for v = 0.4 and fixed memory length L = 50.

Form Figure 5, we noted that when the initial state was changed, there was a rapid interruption in the bifurcation diagrams for of integer order and fractional order. This is also what was observed in bifurcation diagram of fractional map with fixed memory length (Figure 5) when changing the initial value from $x_0 = 0$ to $x_0 = 0.9$.

4 Regular and chaotic behavior of a fractional Gauss map with fixed memory length

In 2003, Gatwald and Melbourne introduced the 0-1 test to prove the existence of chaotic behavior in nonlinear deterministic systems. The 0-1 test is applied to a direct time series and provides a binary-like outcome: A value of $K \approx 0$ indicates regular (nonchaotic) dynamics, while a value of $K \approx 1$ is a strong indicator of chaos. This allows for a clear quantitative distinction between regular and chaotic behavior. The 0-1 test is applied to a direct time series. The 1-0 test can determine the behavior of a given sequence from the dynamics of trajectories p_c and q_c , where a dynamical system is chaotic if the behavior of the trajectories is Brownian motion (k approaches 1), while a dynamical system is regular if the motion is finite (k approaches from 0). For $c \in [0, \pi]$, We have q_c and p_c determined as follows:

$$p_c(n) = \sum_{j=1}^{n} x(j)\cos(jc), \tag{13}$$

$$q_c(n) = \sum_{j=1}^{n} x(j)\sin(jc). \tag{14}$$

The average square displacement $M_c(n)$ of both variables $p_c(n)$ and $q_c(n)$ is calculated from the following relationship:

$$M_c(n) = \frac{1}{N} \sum_{j=1}^{N} (p_c(j+n) - p_c(j))^2 + (q_c(j+n) - q_c(j))^2.$$
 (15)

Finally, we calculate the asymptotic growth rate K using the correlation method, where

$$K = \operatorname{median}(k_c). \tag{16}$$

Also, we have k_c defined by the following relation:

$$k_c = \frac{cov(\xi, \Delta)}{\sqrt{var(\xi)var(\Delta)}} \in [-1, 1], \tag{17}$$

where $\xi = (1, 2, ..., n_{cut}), \Delta = (M_n(1), M_n(2), ..., M_n(cut))$ and $n_{cut} = \text{round}(N/10)$. Moreover, $D_c(n)$ is the adjusted average square displacement.

It has been defined as follows:

$$D_c(n) = M_c(n) - (E(\Phi(x_j)))^2 \frac{1 - \cos(nc)}{1 - \cos(c)},$$
(18)

where the average $E(\Phi)$ is given by

$$E(\Phi(x_j)) = \underline{\lim}_{N \to +\infty} \frac{1}{N} \sum_{j=1}^{N} \Phi(x_j).$$
 (19)

Figure 6 represents the result of the 0-1 test for the fractional Gauss map

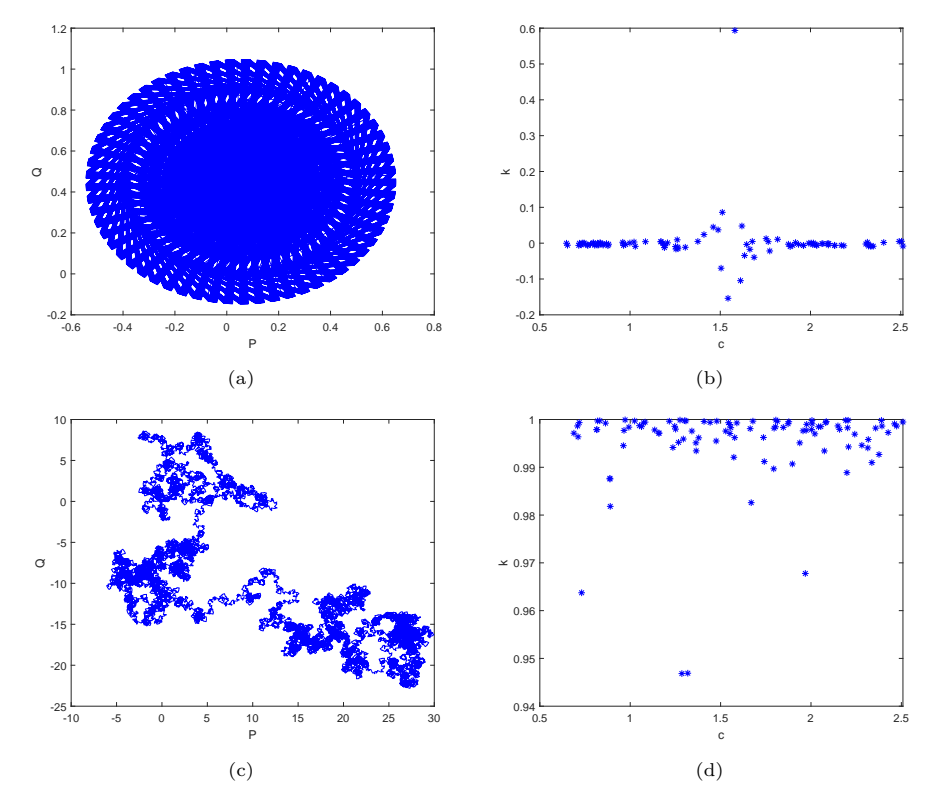


Figure 6: The 0-1 test of fractional Gauss map with fixed memory length $L=50, v=0.4, x_0=0$, (a) (b) for b=0 and (c),(d) for b=-0.7.

where v = 0.4, L = 50 with $x_0 = 0$.

We conducted a 0-1 test at two different values of b. When b=0 the trajectories of p_c and q_c in the (p_c-q_c) plane present bounded (see Figure

6(a)) We also note that the value of k is very close to 0 (see Figure 6(b)), and this translates into a fractional Gauss map with a fixed memory length that non chaotic behavior. When b = -0.7 we note the trajectories of p_c and q_c in the $(p_c - q_c)$ plane, similar to Brownian motion (Figure 6 (c)). We also note that the value of k is very close to 1 (see Figure 6(d)), and this translates into a fractional Gauss map with a fixed memory length that has chaotic behavior.

5 Conclusion

In this study, we proposed a fractional Gauss map with fixed memory length to efficiently model chaotic dynamics. The results demonstrate that the fixedmemory approach can significantly reduce computation time while maintaining the essential features of chaotic behavior.

Unlike traditional infinite-memory fractional systems, the proposed model achieves a balance between memory representation and numerical efficiency, making it more suitable for real-time or large-scale applications.

However, the current study is limited to specific types of chaotic maps and a fixed memory structure. The influence of varying memory lengths, the stability of long-term dynamics, and the accuracy trade-offs require further investigation.

Future work will focus on extending this framework to other fractional maps, exploring adaptive memory strategies, and applying the model to real-world systems such as biological or economic time series. Additionally, more rigorous theoretical analysis of the stability and convergence properties of the fixed-memory fractional model would enhance its mathematical foundation and applicability.

Declarations

Conflicts of Interest: The authors declare no conflict of interest.

Acknowledgements

Authors are grateful to there anonymous referees and editor for their constructive comments.

References

- Abdeljawad, T. On Riemann and Caputo fractional difference, Comput. Math. Appl., 62 (2011), 1602–1611.
- [2] Abdelouahab, M.S. and Hamri, N. The Grünwald-Letnikov fractional-order derivative with fixed memory length, Mediterr. J. Math., 13(2) (2016), 557–572.
- [3] Abdlaziz, M.A.M., Ismail, A. I., Abdullah, F.A. and Mohd, H.M. Bifurcations and chaos in a discrete SI epidemic model with fractional order, Adv. Differ. Equ., 2018 (2018), 1–19.
- [4] Almatrafi, M.B. and Berkal, M. Stability and bifurcation analysis of predator-prey model with Allee effect using conformable derivatives, J. Math. Comput. Sci., 36(3) (2025), 299–316.
- [5] Baleanu, D., Jajarmi, A., Defterli, O., Wannan, R., Sajjadi, S.S. and Asad, J.H. Fractional investigation of time-dependent mass pendulum, J. Low Freq. Noise Vib. Act. Control, 43(1) (2024), 196–207.
- [6] Baleanu, D., Jajarmi, A., Sajjadi, S.S. and Mozyrska, D. A new fractional model and optimal control of a tumor-immune surveillance with non-singular derivative operator, Chaos, 29(8) (2019).
- [7] Baleanu, D., Shekari, P., Torkzadeh, L., Ranjbar, H., Jajarmi, A. and Nouri, K. Stability analysis and system properties of Nipah virus transmission: A fractional calculus case study, Chaos Solitons Fractals, 166 (2023), 112990.
- [8] Bellout, A., Bououden, R., Houmor, T. and Berkal, M. Nonlinear dynamics and chaos in fractional-order cardiac action potential duration

- [9] Bemporad, A. and Morari, M. Control of systems integrating logic, dynamics, and constraints, Automatica, 35(3) (1999), 407–427.
- [10] Berkal, M. and Almatrafi, M.B. Bifurcation and stability of twodimensional activator-inhibitor model with fractional-order derivative, Fractal Fract., 7(5) (2023), 344.
- [11] Berkal, M. and Navarro, J.F. Qualitative behavior of a chemical reaction system with fractional derivatives, Rocky Mt. J. Math., 55(1) (2025), 11–24.
- [12] Bischi, G.I., Gardini, L. and Kopel, M. Analysis of global bifurcations in a market share attraction model, J. Econ. Dyn. Control, 24 (2000), 855–879.
- [13] Bououden, R. and Abdelouahab, M.S. On efficient chaotic optimization algorithm based on partition of data set in global research step, Nonlinear Dyn. Syst. Theory, 18 (2018), 42–52.
- [14] Bououden, R. and Abdelouahab, M.S. Chaos in new 2-d discrete mapping and its application in optimisation, Nonlinear Dyn. Syst. Theory, 20 (2020), 144–152.
- [15] Bououden, R. and Abdelouahab, M.S. Chaotic optimization algorithm based on the modified probability density function of Lozi map, Bol. da Soc. Parana. de Mat., 39 (2021), 9–22.
- [16] Bououden, R., Abdelouahab, M.S. and Jarad, F. Non linear dynamics and chaos in a new 2D piecewise linear map and its fractional version, Electron. Res. Arch., 28 (2020), 505–525.
- [17] Bououden, R., Abdelouahab, M.S., Jarad, F. and Hammouch, Z. A novel fractional piecewise linear map regular and chaotic dynamics, Int. J. General Syst., 50 (2021), 501–526.

- [18] Bourafa, S., Abdelouahab, M.S. and Lozi, R. On Periodic Solutions of Fractional-Order Differential Systems with a Fixed Length of Sliding Memory, J. Innov. Appl. Math. Comput. Sci., 1(1) (2021), 64–78.
- [19] Bouzeraa, S.E.I., Bououden, R. and Abdelouahab, M.S. Fractional logistic map with fixed memory length, Int. J. Gen. Syst., 52 (2023), 653–663.
- [20] Chen, F., Luo, X. and Zhou, Y. Existence Results for Nonlinear Fractional Difference Equation, Adv. Differ. Equ., 2011 (2011), 1–12.
- [21] Crampin, M. and Heal, B. On the chaotic behaviour of the Tent map. An Inter. J. of IMA, 13 (1994), 83–89.
- [22] Dai, W., Zhou, R., Lin, Y. and Liu, Y. Lightweight cryptography for embedded systems—A survey, Sensors, 23(2) (2023).
- [23] Donato, C. and Grassi, G. Bifurcation and chaos in the fractional-ordre Chen system via a time-domain approach, Int. J. Bifurcat. Chaos, 10 (2008), 1845–1863.
- [24] Ebrahimzadeh, A., Jajarmi, A. and Baleanu, D. Enhancing water pollution management through a comprehensive fractional modeling framework and optimal control techniques, J. Nonlinear Math. Phys., 31(1) (2024), 48.
- [25] Gümüş, M. and Türk, K. Dynamical behavior of a hepatitis B epidemic model and its NSFD scheme, J. Appl. Math. Comput., 70(4) (2024), 3767–3788.
- [26] Gümüş, M. and Teklu, S.W. Cost-Benefit and dynamical investigation of a fractional-order corruption population dynamical system, Fractal Fract., 9(4) (2025) 207.
- [27] Gümüş, M. and Türk, K. Global analysis of a monkey-pox virus model considering government interventions, Phys. Scr., 100(4) (2025), 045216.
- [28] Hénon, M. A two dimensional mapping with a strange attractor, Commun. Math. Phys., 50 (1976), 69–77.

- [29] Hilborn, R.C. Chaos and nonlinear dynamics: an introduction for scientists and engineers, Oxford Univ. Press, New York, 2011.
- [30] Hu, T. Discrete chaos in fractional Henon map, Appl. Math., 5 (2014), 2243–2248.
- [31] Jan, C. and Nechvatel, L. Local bifurcations and chaos in the fractional Rossler system, Int. J. Bifurcat. Chaos, 28 (2018), 1850–098.
- [32] Jianping, S., He, K. and Fang, H. Chaos, Hopf bifurcation and control of a fractional-order delay financial system, Math. Comput. Simulat., 194 (2022), 348–364.
- [33] Khennaoui, A.A., Ouannas, A., Bendoukha, S., Wang, X. and Pham, V.T. On chaos in the fractional-order discrete-time unified system and its control synchronization, Entropy, 20 (2018), 530–540.
- [34] Li, T.Y. and Ismail, J.A. Period three implies chaos, Am. Math. Mon., 82 (1975), 985–992.
- [35] Lozi, R. Un attracteur étrange du type attracteur de Hénon, J. Phys., 39 (1978), 9–10.
- [36] Magin, R.L. Fractional calculus in bioengineering, Begell House Publishers, 2006.
- [37] May, R. Simple mathematical models with very complicated dynamics, Nature, 261 (1976), 459–467.
- [38] Miller, K.S. and Ross, B. Fractional difference calculus, Proc. of the International Symposium on Univalent Functions, Koriyama, Japan, 1989, 139–152.
- [39] Sarmah, H.K., Das, M.C., Baishya, T.K. and Paul, R. Chaos in Gaussian map, Int. J. Adv. Sci. Techn. Res., 6 (2016), 160–172.
- [40] Sun, H., Chen, W. and Chen, Y. Variable-order fractional differential models of cardiac action potential, Commun. Nonlinear Sci. Numer., 69 (2019), 354–370.

[41] Wu, G.C. and Baleanu, D. Discrete fractional logistic map and its chaos, Nonlinear Dyn., 75 (2014), 283–287.